Draft version February 1, 2008
Preprint typeset using LaTeX style emulateapj v. 14/09/00

arXiv:astro-ph/0012377v1 18 Dec 2000

A REVISED CEPHEID DISTANCE TO NGC 4258 AND A TEST OF THE DISTANCE SCALE

Jeffrey A. Newman[1], Laura Ferrarese[2], Peter B. Stetson[3], Eyal Maoz[4], Stephen E. Zepf[5], Marc Davis[1], Wendy L. Freedman[6], and Barry F. Madore[6,7]
jnewman@astro.berkeley.edu, lff@physics.rutgers.edu, Peter.Stetson@hia.nrc.ca, maoz@ism.arc.nasa.gov, zepf@astro.yale.edu, marc@astro.berkeley.edu, wendy@ociw.edu, barry@ipac.caltech.edu

Draft version February 1, 2008

ABSTRACT

In a previous paper (Maoz *et al.* 1999), we reported a Hubble Space Telescope (HST) Cepheid distance to the galaxy NGC 4258 obtained using the calibrations and methods then standard for the Key Project on the Extragalactic Distance Scale. Here, we reevaluate the Cepheid distance using the revised Key Project procedures described in Freedman *et al.* (2001). These revisions alter the zero points and slopes of the Cepheid Period-Luminosity (P-L) relations derived at the Large Magellanic Cloud (LMC), the calibration of the HST WFPC2 camera, and the treatment of metallicity differences. We also provide herein full information on the Cepheids described in Maoz *et al.* 1999. Using the refined Key Project techniques and calibrations, we determine the distance modulus of NGC 4258 to be 29.47 ± 0.09 mag (unique to this determination) ± 0.15 mag (systematic uncertainties in Key Project distances), corresponding to a metric distance of $7.8 \pm 0.3 \pm 0.5$ Mpc and 1.2σ from the maser distance of 7.2 ± 0.5 Mpc. We also test the alternative Cepheid P-L relations of Feast (1999), which yield more discrepant results. Additionally, we place weak limits upon the distance to the LMC and upon the effect of metallicity in Cepheid distance determinations.

1. INTRODUCTION

Distances to other galaxies obtained by observations of Cepheid variables with the Hubble Space Telescope (HST) lie at the core of most recent efforts to determine the extragalactic distance scale. The small observed scatter in the relationship between Cepheids' pulsation periods and luminosities, their large numbers (which allow many independent measures of the distance to a galaxy), and the simplicity of the basic physics underlying their variability all have made them uniquely suitable for this purpose. As a consequence of their integral role in establishing the distance scale, however, any changes in the calibration and application of the Cepheid period–luminosity (P–L) relationship will affect many other secondary methods of distance measurement. Any improvements in techniques for obtaining Cepheid distances are thus extremely valuable; but this also means that any changes in this vital link should be well scrutinized if they are to be adopted.

In a paper describing the final results of the HST Key Project on the Extragalactic Distance Scale (henceforward, the Key Project), Freedman *et al.* (2001) make a number of refinements to the techniques used in earlier papers in the series based upon newly-available information. First and foremost, microlensing experiments (e.g., Udalski *et al.* 1999) and dedicated efforts (Sebo *et al.* 2001) have greatly enlarged the set of calibrating LMC Cepheids beyond what had been studied when the initial Key Project P–L relation was determined (Madore & Freedman 1991). The resulting samples have revealed a modest correction to the previously adopted P–L slope for I observations; the V–band slope remains unchanged. In the Key Project methodology, Cepheid magnitudes are corrected for extinction using their observed color excess $E(V-I) = (V-I) - (V-I)_0$, where $(V-I)_0$ is the expected color of an unreddened Cepheid of given period based upon the LMC–calibrated P–L relations. This procedure is sensitive to the reddening, since $A_V = 2.45 \times E(V-I)$). An error in the P–L slope in I thus propagates into a larger, period–dependent error in the true distance modulus; in this case, $\Delta\mu_0 = -0.24(\log_{10} P - 1)$. Because in more distant galaxies only brighter, longer-period Cepheids are observable, this generally results in a distance-dependent revision to HST Cepheid distances which in extreme cases can reach -0.20 mag. Further details are given in Freedman et al. (2001).

Second, our understanding of charge transfer efficiency and related effects in the WFPC2 CCDs has greatly improved in recent years (e.g., Stetson 1998, Dolphin 2000), motivating revisions in the Hill *et al.* (1998) photometric zero points used in most ear-

[1] Department of Astronomy, University of California, Berkeley, CA 94720
[2] Rutgers University, New Brunswick, NJ, 08854
[3] Dominion Astrophysical Observatory, 5071 W. Saanich Rd., Victoria, B.C., Canada V8X 4M6
[4] NASA Ames Research Center, MS 245-3, Moffett Field, CA 94035-1000
[5] Department of Astronomy, P.O. Box 208101, Yale University, New Haven, CT 06520
[6] Observatories of the Carnegie Institution of Washington, 813 Santa Barbara St., Pasadena, CA 91101
[7] NASA/IPAC Extragalactic Database, Infrared Processing and Analysis Center, Jet Propulsion Laboratory, California Institute of Technology, MS 100-22, Pasadena, CA 91125

lier Key Project papers. Freedman *et al.* adopt the calibration of Stetson (1998), which results in a -0.02 mag mean adjustment in V and -0.04 mag in I from the Hill "long" zero points. Carrying this through the Key Project procedures for obtaining reddening-corrected distance moduli, they apply a net correction of -0.07±0.07 mag to distances obtained using the Hill "long" zero point (where the error adopted reflects a conservative estimate of systematic differences among recent calibrations).

The third change made in the revised Key Project procedures is the adoption of Cepheid distance moduli adjusted for metallicity effects as standard. The typical metallicity of Cepheids in the LMC with which the P–L relation is calibrated differs by ~ 0.5 dex from that in many of the fields observed in the course of the Key Project. Metallicity differences may produce measurable differences in the colors and magnitudes of Cepheids in those fields from ones found in the LMC; unfortunately, neither theoretical calculations (as those of Alibert *et al.* 1999 or Musella 1999) nor observations (cf. Kennicutt *et al.* 1998, Sasselov et al. 1997, Kochanek 1997, or Nevalainen & Roos 1998) have provided a definitive determination of the magnitude, or even sign, of this effect. Freedman *et al.* (2001) adopt a correction to Cepheid magnitudes of -0.2 ± 0.2 mag/dex (based upon current observational results) as standard. In previous Key Project work, distance moduli uncorrected for metallicity effects were primarily used, though results for a correction of -0.24 mag/dex were also given. In their error budget, Freedman *et al.* estimate the potential systematic error in a typical Key Project Cepheid distance measurement due to corrections for differences in metallicity from the LMC to be ±0.08 mag.

Even with these revisions, important uncertainties remain in the Cepheid-calibrated distance scale. Foremost among these is the distance to the Large Magellanic Cloud (LMC), using which the Key Project Period–Luminosity relation has been calibrated. A wide variety of measurements of the distance to the LMC have been performed in the past few years. Many of these studies disagree with each other statistically, spanning roughly 0.5 mag in distance modulus. Freedman *et al.* (2001) adopt 18.50 ± 0.10 mag as the distance modulus of the LMC; the uncertainty in the LMC distance modulus leads directly to a systematic uncertainty in the Cepheid distance scale of ±0.10 mag. After the uncertainties in the LMC distance and metallicity corrections, the next most significant contribution to the Key Project systematic error budget is the difficulty in determining zero points for WFPC2 photometry, which is estimated to lead to a ±0.07 mag uncertainty in HST Cepheid distance moduli; a variety of other systematic effects could enter at lower levels.

Given the remaining uncertainties, it is worthwhile to test the revised Key Project distance scale using a galaxy with a well-known, primary distance and with a metallicity typical of galaxies observed in the course of the Key Project. To be useful, such a test requires that Cepheids be observed with the same instruments, filters, and parameter measurement techniques as used for objects in the Key Project sample. Such a test has already been applied to the original Key Project distance scale based upon observations of Cepheids in NGC 4258 (Maoz *et al.* 1999).

The spiral galaxy NGC 4258 (SABbc, $M_B = -20.0$ mag) presents a unique opportunity for such a test because of the precision with which its distance has been measured in a manner independent of the conventional ladder of astronomical distance scales (Freedman 1998). Furthermore, its metallicity and distance are similar to those of typical targets of HST Cepheid programs. The distance to NGC 4258, 7.2 Mpc (corresponding to distance modulus 29.28 mag), has been determined using its apparently simple, Keplerian circumnuclear disk delineated by line-emitting water masers that orbit a supermassive black hole at its center (Miyoshi *et al.* 1995, Maoz 1995).

This disk was discovered by VLBI observations of water maser emission from the central region of the galaxy (Miyoshi *et al.* 1995). It is about 16 mas in diameter, $\lesssim$0.1 mas in thickness, rotates at speeds of $\approx 10^3$ km s^{-1}, and is viewed by us from nearly edge-on. Most remarkably, the rotation curve of the maser sources is Keplerian to high precision ($\lesssim$0.5%), which provides very strong evidence for a supermassive black hole at the galaxy center (Maoz 1995). The high angular resolution (0.2 mas) and spectral resolution (0.2 km s^{-1}) of VLBA observations (Moran *et al.* 1995) allow a precise definition of the disk structure and kinematics. Combining the observed rotation velocities with the measured centripetal acceleration in the disk (Greenhill *et al.* 1995) or with the observed proper motions of the maser sources (Herrnstein *et al.* 1999) permits independent measurements of the physical size of the disk; comparing these to its observed angular extent yields the distance to the galaxy via simple geometry. These distance measurements are subject to only small uncertainties. The differential systematic error in the maser positions is $\lesssim$0.04 mas (Moran *et al.* 1995), translating into a relative distance error smaller than 0.5%. The distance to the masing disk scales with the disk's inclination as $(\sin i)^{-1}$; since the disk is viewed nearly edge-on, $i = 83° \pm 2°$ (Herrnstein *et al.* 1996), an error even as high as 4° would introduce a distance error of only 1%. Relativistic corrections due to gravitational redshift and transverse Doppler shift have been taken into account and are much smaller. The disk is slightly warped, but the distance determination is not sensitive to the warp model adopted. The warp contributes, though, to the small uncertainty in the disk inclination mentioned above. The total estimated uncertainty in this distance is ±0.3 Mpc if the disk is presumed to be circular (which it appears to be to better than 0.5%). If nonzero eccentricities are allowed, the uncertainty increases to ±0.5 Mpc

(we adopt this more conservative value for all further discussions). The direct, geometric methods used are believed to have minimal unknown systematic uncertainties. The two routes to a distance (proper motions and accelerations) yield results in agreement with each other to 1%.

As described in Maoz *et al.* (1999), we have therefore obtained and analyzed HST observations of NGC 4258 with the intention of testing, and potentially of better determining, the zero point of the Cepheid P-L relation. In that work, we used the then-standard Key Project methodologies and calibrations, and found a $\geq 1.3\sigma$ discrepancy between the HST Cepheid distance and that obtained from studies of the masing disk. In this paper, we perform a similar test after obtaining a Cepheid distance using the revised Key Project procedures, allowing an evaluation of the new techniques. We also provide herein full information (locations, light curves, finding charts, etc.) for the Cepheids described in Maoz *et al.* 1999. We present the observations, the reduction of the data and the search for Cepheids in §2, the resulting derivation of a Cepheid distance in §3, and the implications in §4.

2. OBSERVATIONS, DATA REDUCTION, AND SEARCHES FOR VARIABLE STARS

We observed a portion of NGC 4258 using the Wide Field and Planetary Camera 2 (WFPC2) instrument and the Hubble Space Telescope on 11 epochs in 1998. The data were acquired with an optimal power-law spacing between them as described in Freedman *et al.* (1994) and Madore & Freedman (2001). The $F555W$ and $F814W$ filters were used for a combined total of one orbit at every epoch, with two frames obtained using each filter to limit the effects of cosmic rays; the exposure time per frame was 500 seconds. A journal of observations is given in Table 1. To simplify analysis, a fixed orientation was maintained for all epochs. The field observed is superimposed on a ground-based image of NGC 4258 in Fig. 1.

2.1. *Photometric Reductions*

We have obtained photometry from these data with two commonly-used software packages: DAOPHOT/ALLFRAME and DoPHOT. For both analyses, the data were first preprocessed via the standard Space Telescope Science Institute pipeline (Holtzman *et al.* 1995). For the ALLFRAME photometry each frame was also corrected for vignetting and geometrical effects on the effective pixel area as described in Stetson *et al.* (1998). Photometry was then performed on each of the data frames using the DAOPHOT II/ALLFRAME package (Stetson 1987). ALLFRAME fits a predefined point-spread function (PSF) to all stars on a frame and iteratively determines their magnitudes. The procedures used throughout were similar to those of the Key Project (see Stetson *et al.* 1998). The photometric zero points of Stetson (1998) were used. Aperture corrections for each frame were derived using a set of bright, isolated stars.

In addition to the Cepheid analysis described below, we also attempted to determine a tip of the red giant branch (TRGB) distance (Lee *et al.* 1993) to NGC 4258 using the ALLFRAME photometry for WF2 and WF3. However, our observations were insufficiently deep and contamination by other stellar populations too great to allow any convincing detection of the TRGB.

The DoPHOT photometry was performed using a variant of the DoPHOT package (Schechter *et al.* 1993, Saha *et al.* 1994) which was developed especially to deal with the photometry of undersampled images such as those obtained with the HST. In addition to the data processing mentioned earlier, pairs of cosmic ray split images were combined prior to performing the photometric reduction with DoPHOT. The algorithm used for this is designed to reject cosmic ray events; particular care is taken to ensure that the photometry of real objects is preserved. Further discussion of the application of DoPHOT to photometry of HST images can be found in Saha *et al.* (1996a), Ferrarese *et al.* (1996, 1998), and Hill *et al.* (1998).

The photometric calibration adopted again follows Stetson (1998), as per the revised Key Project procedures of Freedman *et al.* (2001). The limited number of bright, uncrowded stars prevented us from deriving reliable spatially-dependent aperture corrections for DoPHOT. We therefore adopted corrections obtained from observations of an uncrowded field in the Leo I dwarf galaxy. Aperture photometry conducted on the NGC 4258 individual frames, as well as on a deep frame obtained by combining all available epochs, produces results in agreement with the Leo I aperture corrections at the 0.03 mag level, which we therefore adopt as a measure of the uncertainty in the correction themselves.

2.2. *Variable Star Searches*

Searches for Cepheid variables using the ALLFRAME photometric measurements were conducted using two different algorithms. One of these selects candidate variables via a modified Welch-Stetson test and performs a nonlinear fit of template Cepheid light curves to their photometry to assess their variability and determine their parameters; see Stetson (1996) and Stetson *et al.* (1998) for further description. The other linearly fits template light curves defined on a grid in period and phase to all stars with well-determined photometry; Cepheids are then identified by a set of criteria that are effective at eliminating nonvariables. This algorithm is described in more detail in Newman et al. (1999). Both searches independently yielded similar sets of candidate Cepheid variables and parameter estimates in good agreement. These algorithms in combination yielded 21 potential Cepheid variables.

A search for variable stars was also conducted using DoPHOT magnitude measurements for the V and $I-$band frames independently following the

procedure described by Saha & Hoessel (1990). We required that a star be detected at at least 8 of the 11 epochs in order to be checked for variability. We also excluded all stars in crowded regions by rejecting candidates that had a companion contributing more than 50% of the total light within a two-pixel radius. A detailed discussion of the search procedure can be found in Ferrarese *et al.* (1996). A star meeting the above constraints was flagged as a variable if $\chi^2_r \geq 8$ or $\Lambda \geq 3$ where χ^2_r and Λ are as used in Saha & Hoessel (1990).

Several spurious variables were detected by this procedure as a consequence of non-Gaussian sources of error and various anomalies in the images (e.g., residual cosmic ray events) along with the crowding referred to earlier. Each variable star candidate was visually inspected by blinking several of the individual frames against each other. The best period for each variable was selected by phasing the data for all periods between 3 and 60 days in incremental steps of 0.1 days. Although in most cases the adopted period corresponds to a minimum value of the phase dispersion, in a few cases an obvious improvement of the light curve was obtained for a slightly different period. The DoPHOT analysis identified a total of 28 potential Cepheids.

2.3. *DoPHOT-ALLFRAME Comparison*

All Cepheids found in either dataset were on Wide Field (WF) chips 2 or 3; we therefore will restrict our discussion to these for the remainder of this paper. On WF2, the agreement of DoPHOT and ALLFRAME results was well within the expected errors in the aperture corrections used; the mean difference between ALLFRAME and DoPHOT magnitudes for 24 bright, isolated stars was 0.026 ± 0.049 (standard deviation; standard error of the mean 0.009) mag for V, and 0.015 ± 0.049 mag for I. For WF3, the mean difference for 30 stars was 0.025 ± 0.027 mag for V, and 0.088 ± 0.046 mag for I. Mean magnitudes for Cepheids yielded results consistent with these to within 1σ, albeit with much larger standard errors due to their fainter magnitudes.

We believe that the WF3/I results are an aberration closely related to the discrepant distance moduli obtained from ALLFRAME magnitudes on the two chips (q.v. § 3). This anomoly is plausibly accounted for by the difficulties of determining aperture corrections in the observed fields, which contain few bright, isolated stars. If we presume that this is the case, the WF3/I ALLFRAME photometry may be corrected by bringing it onto the same system as the WF2 and WF3/V ALLFRAME magnitudes; i.e., adjusting the WF3/I ALLFRAME magnitudes to be 0.022 ± 0.0035 mag fainter than DoPHOT (the average difference from the other three chip/filter combinations), rather than 0.088 ± 0.008 mag without any correction. Averaging the ALLFRAME-DoPHOT differences from those three cases may be justified by the fact that errors in aperture corrections, etc. are generally highly correlated between V and I and from one WF chip to another; and indeed, the ALLFRAME-DoPHOT offsets for WF2/V and I and WF3/V are all quite consistent, agreeing to within 0.01 mag. Therefore, in addition to presenting results for unmodified ALLFRAME photometry, in the next section we also provide distance measurements obtained from ALLFRAME data "corrected" by subtracting 0.066 ± 0.009 mag from WF3/I magnitudes.

3. THE CEPHEID P-L RELATIONS

We have identified and determined light curves, periods, mean magnitudes, and colors for 15 definitive Cepheids in NGC 4258. All of these stars fulfill four criteria: they are identified as variable by all three search techniques, they fit a Cepheid template light curve with reasonable χ^2, they visibly vary in blink comparisons in both $F555W$ and $F814W$ images, and they have negligible statistical probability of being misidentified nonvariables.

A variety of methods exist for determining the mean magnitudes of Cepheids. In this paper, we use the intensity-weighted mean magnitude obtained from a fit to the Cepheid light curve using the templates of Stetson (1996), also known as "template fit" mean magnitudes. This is the preferred method for the Key Project, providing a robust method of determining mean magnitudes analogous to those obtained for more densely sampled datasets (such as the LMC Cepheids used for calibrating the P–L relation). We note that adopting other standard magnitude averaging methods changes the NGC 4258 distance modulus obtained by no more than 0.04 mag. We use the Cepheid periods determined in the DoPHOT analysis for all distance modulus calculations, as these yielded smaller scatter about the P–L relation for all datasets and averaging methods than alternatives (e.g., periods determined from template fits), likely reflecting the fact that those periods were refined by hand when necessary to improve the Cepheid light curves, rather than being determined solely by an automated algorithm. We have adopted the DoPHOT photometry for all major conclusions reported here, since as discussed in § 3, ALLFRAME photometry yielded internally discrepant distances from Cepheids on the two WFPC2 chips used; however, as an additional consistency check we also provide ALLFRAME values in much of what follows. We present the locations and characteristics of the Cepheids found in Table 2, and complete DoPHOT photometry for those stars in Table 3. The positions of the Cepheids are shown in Fig. 2, and detailed finding charts may be found in Fig. 3. DoPHOT light curves for the Cepheids found are depicted in Fig. 4.

In accordance with the revised Key Project methodology, we adopt the P-L relation slopes of Freedman *et al.* (2001) and only fit for differences in the zero point. Their LMC calibration yields mean absolute magnitudes for Cepheids

$$\bar{M_V} = -2.760(\pm 0.03)(\log_{10} P - 1) - 4.218(\pm 0.02) \quad (1)$$

$$\bar{M}_I = -2.962(\pm0.02)(\log_{10} P - 1) - 4.904(\pm0.01),$$

where $\bar{M}_V$ and $\bar{M}_I$ are the intensity-weighted mean absolute Johnson V and Kron-Cousins I magnitudes of the star and P is its period in days. The same relations have been used by Freedman *et al.* (2001) and Macri *et al.* (2001). Fitting the observed magnitudes of Cepheids in NGC 4258 with such relations yields a measurement of the apparent distance modulus of the galaxy. We have done this fitting with the standard Key Project processor, which determines overall distance moduli as an unweighted mean of the values for individual stars. From the difference between the absolute magnitudes of LMC Cepheids (for an assumed LMC distance modulus of 18.50 mag) and the observed magnitudes of NGC 4258 Cepheids we then may derive a V or I distance modulus to NGC 4258. We present the resulting distance moduli for both ALLFRAME and DoPHOT photometry in Table 4, both for the entire sample and the subsets of Cepheids on either Chip 2 or Chip 3 (which can indicate the presence of catastrophic photometric or other errors). The DoPHOT NGC 4258 P-L relations are plotted in Figure 5, and those from ALLFRAME in Figure 6.

In Key Project procedures, the colors of the observed Cepheids (compared to those of a calibration set of such stars in the LMC whose reddening has been assumed) are then used to correct for line-of-sight of extinction assuming a Cardelli *et al.* (1989) reddening law. This may be done by comparing the distance moduli obtained in the V and I bands; the difference of the two measures the average value of $E(V-I)$. Because the Key Project processor uses only unweighted averages with no rejection, this is equivalent both to applying the extinction correction star-by-star and then averaging and to fitting the P-L relation for a reddening-corrected "Wesenheit" magnitude, $\bar{W} = \bar{V} - 2.45(\bar{V} - \bar{I})$ (Madore 1982, Madore & Freedman 1991). This method yields $E(V-I) = 0.20\pm0.04$ mag and an extinction-corrected distance modulus of $\mu_0 = 29.40\pm0.06$ mag from DoPHOT photometry for all Cepheids; for the ALLFRAME photometry, the corresponding numbers are 0.19 ± 0.04 and 29.53 ± 0.07 mag. The true moduli for the subset of Cepheids on either WF2 or WF3 are also listed in Table 4. Note that in the ALLFRAME dataset, Cepheids on the two chips yield extinction-corrected distance moduli differing by 0.25 mag, or 1.9σ; the DoPHOT moduli differ by only 0.07 mag (0.5σ). Furthermore, the value for WF2 is quite consistent with that obtained from DoPHOT photometry, both for single chips' samples and overall; this makes the WF3 ALLFRAME results particularly suspect.

The bulk of this discrepancy is eliminated if we perform the WF3/I correction described in § 2.3. That adjustment of WF3/I magnitudes by 0.066 ± 0.009 mag reduces the overall distance modulus yielded by Cepheids on WF3 by 0.162 ± 0.021 mag. Such a correction reduces the ALLFRAME WF2/WF3 discrepancy to 0.09 mag, a 0.7σ difference. As seen in Table 4, this correction would leave ALLFRAME V distance moduli unchanged, alter the WF3 and overall average I moduli to 29.77 mag, and reduce the extinction-corrected distance modulus to 29.48 ± 0.09 mag for WF3, or 29.44 ± 0.065 mag overall (where the errors include the propagated error from the uncertainty in the ALLFRAME-DoPHOT differences, 0.021 mag, added in quadrature). These values are in much better agreement with those obtained from DoPHOT photometry (for which the overall, extinction-corrected distance modulus was $\mu_0 = 29.40 \pm 0.06$ mag). Applying this correction also reduces the scatter in the overall, extinction-corrected ALLFRAME distance modulus from 0.35 mag to 0.25 mag.

Freedman *et al.* (2001) find that differences in metallicity have an effect on extinction-corrected Cepheid distances of 0.2 ± 0.2 mag/dex. Using the fits to data on NGC 4258 HII regions from Zaritsky, Kennicutt, and Huchra (1994), we estimate the metallicity in our HST fields to be $12+\log(\mathrm{O/H})=8.85\pm0.06$, 0.35 dex higher than that adopted for Cepheids in the LMC. This leads to a correction of $+0.07\pm0.07$ mag to the distance moduli we have derived. The revised Key Project procedures adopt metallicity-corrected values for the distance modulus as their primary estimate (in contrast to previous practice); we thus do likewise, and obtain a final true modulus to NGC 4258 of 29.42 mag. Because the metallicity of NGC 4258 is quite typical of Key Project targets, we treat the uncertainty in the metallicity correction as a systematic uncertainty in the distance scale.

3.1. *Uncertainties*

We present an error budget for our measurement of the distance to NGC 4258 in Table 5. In addition to the random errors determined in the course of fitting P–L relations, uncertainties in the aperture corrections used are also random between different Cepheid target galaxies. From studies of globular clusters and Key Project galaxies, we expect these to be approximately 0.05 magnitude or less in both V and I, and highly correlated between the two bands; the combined uncertainty due to the aperture corrections in the reddening-corrected distance modulus would then still be 0.05 mag. Differences between ALLFRAME and DoPHOT photometry of bright stars are much smaller than this in all cases save WF3/I. Since it appears that the difference between the overall DoPHOT and uncorrected ALLFRAME distance primarily reflects a correctable error in the WF3/I ALLFRAME photometry alone, we estimate that photometric errors in the DoPHOT results which are unique to our study of NGC 4258 may constitute 0.05 mag. Adding all potential sources in quadrature, the total random uncertainty in our determination of a Cepheid distance to NGC 4258 (R_{tot} in Table 5) is 0.09 magnitude.

This measurement is also subject to a number

of potential sources of systematic error that affect Key Project distance determinations similarly, as described in Table 5; their possible contributions have been estimated to total ±0.15 mag (Ferrarese *et al.* 1999, Freedman *et al.* 2001). For those potential systematic errors which affect all Cepheid distances obtained in the same manner as ours uniformly, we have adopted the uncertainty estimates of the Key Project (Freedman *et al.* 2001); more detailed descriptions may be found therein.

We thus obtain a Cepheid distance modulus to NGC 4258 of 29.47 ± 0.09 mag (unique to this determination) ±0.15 mag (systematic uncertainties in Key Project distances), corresponding to a metric distance of 7.8 ±0.3 Mpc ±0.5 Mpc. When treated in the same way, the uncorrected ALLFRAME results yield a distance modulus of 29.60 ± 0.10 mag, corresponding to a metric distance of 8.3 ± 0.4 Mpc, while the corrected ALLFRAME results yield a distance modulus of 29.51 ± 0.09 mag, corresponding to a metric distance of 8.0 ± 0.3 Mpc. The distance to NGC 4258 derived from observations of Cepheids using the revised Key Project methodologies is thus not significantly greater than the maser distance of 7.2 ± 0.5 Mpc (Herrnstein *et al.* 1999).

4. IMPLICATIONS

In assessing the validity of the calibration of the Cepheid distance scale using NGC 4258, we must consider how significant the difference we have found is. First of all, we may examine whether the differences are consistent within the random and systematic error budgets of the two processes; i.e., whether previously considered sources of error are sufficient to account for what we have found. The Cepheid and maser distances differ by 0.9σ if we add in quadrature our measurement uncertainty of 0.3 Mpc, the Key Project systematic error estimate of 0.5 Mpc, and the maser distance error estimate of 0.5 Mpc; potential systematic errors in either technique do not appear to have been underestimated. In performing a test of the validity of the revised Key Project distance scale, however, we must consider what sort of a discrepancy we can measure. All HST Cepheid distances following the revised techniques will share the systematic errors that affect our results. Thus, we should consider only the random errors unique to this measurement and those errors affecting the maser distance in determining whether a recalibration would be an improvement. In that case, we find a 1.2σ difference, as opposed to a 1.6σ difference if the results of Maoz *et al.* (1999) were evaluated with the same error budget. Put differently, if we were to presume the maser distance to NGC 4258 is correct and recalibrate the distance scale based upon our Cepheid observations of NGC 4258, all revised Key Project distances would have to be reduced by 0.19 mag, increasing the resulting measurements of the Hubble constant by 10%; the total systematic error budget for the new calibration would be 0.16 mag (8%), slightly greater than that resulting from the current, LMC-based methods. Modest changes in calibration or methodology would be sufficient to bring the Cepheid and maser distances into substantially better agreement; for instance, the LMC distance need only be reduced by a few hundredths of a magnitude, well within the Key Project estimate of its uncertainty, to bring the difference below 1σ.

We can similarly use our measurement of the distance to NGC 4258 to test other calibrations of the Cepheid P-L relation. In particular, we have applied the Milky Way-based calibration of Feast (1999), which corresponds to:

$$\bar{M}_V = -2.81(\pm 0.06)(\log_{10} P - 1) - 4.26(\pm 0.05) \quad (2)$$
$$\bar{M}_I = -3.07(\log_{10} P - 1) - 4.89,$$

following the conventions of equation 1. Note that the slopes adopted in deriving these relations are substantially different from those used by Freedman *et al.* (2001). Although the Cepheids in Feast's calibration are not at uniform distance, making their use to calibrate the P-L relation somewhat more complicated, they are independent of any assumptions about the LMC distance and of very similar metallicity to the fields we have studied. Using these relations leads to a Cepheid distance modulus for NGC 4258 of 29.51 ± 0.06 (random) mag, 0.23 mag greater than the maser result; a metallicity correction of -0.2 mag/dex increases this by only 0.01 mag. This is a total discrepancy of 1.3σ if we consider all possible errors and assume a systematic uncertainty of 0.05 mag in Feast's calibration, 1.2σ for 0.1 mag, or 1σ for 0.15 mag uncertainty. If, as above, we compare the discrepancy to what we can measure, we find that the maser and Cepheid distances are 1.5σ apart; the calibration of Feast (1999) might be improved by rereferencing it to NGC 4258.

Some authors (e.g. Gibson 2000) have used the results of Maoz et al. (1999) to estimate the distance to the Large Magellanic Cloud, based upon the assumption that the maser distance to NGC 4258 is correct and that any differences between the Cepheid distance to that galaxy and the maser distance are due to an error in the distance to the LMC assumed in calibrating P–L relations. Such a procedure is subject to many sources of uncertainty; the random uncertainty in the resulting LMC distance will correspond to the sum in quadrature of the random uncertainties in the maser and Cepheid distances to NGC 4258. Furthermore, the uncertainty due to potential systematic errors in that procedure includes contributions from all possible systematics in the maser and Key Project error budgets, save the distance to the LMC itself. If we nevertheless proceed in this manner, we determine an LMC distance modulus of 18.31 ± 0.11 (random) ± 0.17 (systematic).

Similarly, we may use the maser and Cepheid distances to NGC 4258 to place limits on the effect of metallicity on Cepheid luminosities. In that case, we should consider all random and systematic uncertainties in the maser or Cepheid distances save

those due to metallicity effects; they total 0.21 mag. Thus, the Cepheid distance becomes 1σ discrepant from the maser distance if there is a total metallicity correction of +0.09 mag to the uncorrected Cepheid distance, and 2σ discrepant with a correction of +0.30 mag. As the metallicity of NGC 4258 is 0.35 ± 0.06 dex greater than that of the LMC, we thus can limit the effect of metallicity on Cepheid mean magnitudes to -0.26 mag/dex at 1σ, or -0.9 mag/dex at 2σ.

NGC 4258 has provided the most stringent geometrical test of the revised Key Project distance scale so far. The 0.26 mag discrepancy between the maser distance and the Cepheid distance to NGC 4258 obtained with the original Key Project methods diminishes to 0.19 mag when the revisions of Freedman *et al.* (2001) are applied. This provides one piece of evidence that the changes made to the Key Project distance scale are, in fact, improvements. A stronger test of the HST Cepheid distance scale based on the maser distance to NGC 4258 would require a substantially larger sample of Cepheids (which should reduce the uncertainties in determining the VI P–L relations and the reddening) and better determination of aperture corrections; these issues can be addressed simultaneously by searching for Cepheids with HST in a field that contains more stars and has undergone more recent star formation, preferably with the higher resolution that will be afforded by the Advanced Camera for Surveys. It would be reasonable to expect that observations of a region richer in Cepheids might yield as many as 3 times the number of Cepheids (giving a distance modulus uncertainty of 0.04 magnitude) and aperture corrections accurate to ± 0.04 magnitude; better agreement between ALLFRAME and DoPHOT analyses might also occur with improved data. Reductions of uncertainties in the maser distance (e.g., via improved constraints on the eccentricity of the circumnuclear disk), would also be greatly beneficial for its use to calibrate the extragalactic distance scale. Successful maser distances to other galaxies, establishing a Hubble relation, would more firmly establish this novel and promising technique. The data available at present are sufficient only to test calibrations of the extragalactic distance scale, but that alone is of great value. With improvements in both Cepheid and maser analyses, NGC 4258 has great potential for establishing a new primary step in the distance ladder, reducing the potential systematic errors in measurements of the Hubble constant to perhaps as little as 5%, and bypassing controversies over the distance to the Large Magellanic cloud and the effect of metallicity on the colors and magnitudes of Cepheids entriely.

We would like to thank Bryan Mendez for his assistance in attempting a TRGB measurement of the distance to NGC 4258 and our referee and editor for their helpful suggestions. This work was supported by NASA grant GO-07227 from the Space Telescope Science Institute (operated by AURA, Inc. under NASA contract NAS 5-26555).

REFERENCES

Bartel, N. *et al.* 1999, BAAS, 194.6208
Cardelli, J.C., Clayton, G.C. & Mathis, J.S. 1989, Ap. J., 345, 245
Dolphin, A. E. 2000, PASP, 112, 1397
Eastman, R.G., Schmidt, B.P., & Kirschner, R. 1996, Ap. J., 466, 911
Feast, M. 1999, PASP, 111, 775
Ferrarese, L. *et al.* 1998, Ap.J., 464, 568
Ferrarese, L.F. *et al.* 2000, Ap. J., 529, 745
Freedman, W.L. 1997, in *Critical Dialogues in Cosmology*, ed. N. Turok (World Scientific, Singapore), 92
Freedman, W.L. 1998 in *Relativistic Astrophysics and Cosmology*, eds. A. V. Olinto, D.N. Schramm, & J.A. Frieman (World Scientific, Singapore)
Freedman, W.L. 1999, *Particle Physics and the Universe* (World Scientific Press, Singapore)
Freedman, W.L. *et al.* 2001, ApJ, submitted
Freedman, W.L. *et al.* 1994, Ap. J., 427, 628
Gibson, B. K. 1999, astro-ph/9910547, preprint
Gould, A. & Uza, O. 1998, Ap. J., 494, 118
Greenhill, L.J., Henkel, C., Becker, R., Wilson, T.L., & Wouterloot, J.G.A. 1995, A&A, 304, 21
Hedges, L.V. 1985, *Scientific Methods of Meta-Analysis* (Academic Press, Orlando)
Herrnstein, J.R. *et al.* 1999, Nature, 400, 539
Kennicutt, R.C. Jr., Freedman, W.L., & Mould, J.R. 1995, A.J., 110, 1476
Kennicutt, R. C. Jr. *et al.* 1998,Ap. J., 498, 181
Krauss, L. M. 1998, Ap. J., 501, 461
Jacoby, G.H. *et al.* 1992, PASP 104, 599
Lee, M.G., Freedman, W.L., & Madore, B.F. 1993, ApJ, 417, L553
Macri, L. *et al.* 2001, ApJ, approved
Madore, B.F. & Freedman, W.L. 1991, PASP, 103, 933
Madore, B. F. *et al.* 1999, Ap. J., 515, 29
Maoz, E. 1995 Ap.J., 494, L181
Maoz, E. *et al.* 1999, Nature, 401, 351
Miyoshi *et al.* 1995, Nature, 373, 127
Mould, J.R. *et al.* 2000, Ap.J., 529, 786
Newman, J.A. *et al.* 1999, Ap.J., 523, 506
Panagia, N. 1999 in *New Views of the Magellanic Clouds*, eds. Y.H. Chu, N.B. Suntzeff, J.E. Hesser, & D. Bohlender (A.S.P., San Francisco)
Saha, A., Labhardt, L., Schwengeler, H., Macchetto, F.D., Panagia, N., Sandage, A., & Tammann, G.A. 1994, Ap.J., 425, 14
Sakai, S. *et al.* 2000, Ap. J., 529, 698
Schechter, P.L., Mateo, M., & Saha, A. 1993, PASP, 105, 1342
Stetson, P.B. 1994 PASP, 106, 250
Stetson, P. B. 1996, PASP, 108, 851
Stetson, P.B. *et al.* 1998, Ap.J., 508, 491
Zaritsky, D., Kennicutt, R.C. Jr., & Huchra, J.P. 1994, Ap. J., 420, 87

FIG. 1.— A 13′ × 13′ Digital Sky Survey image of NGC 4258, with the field observed using HST superimposed. North is oriented vertically and East to the left in this image.

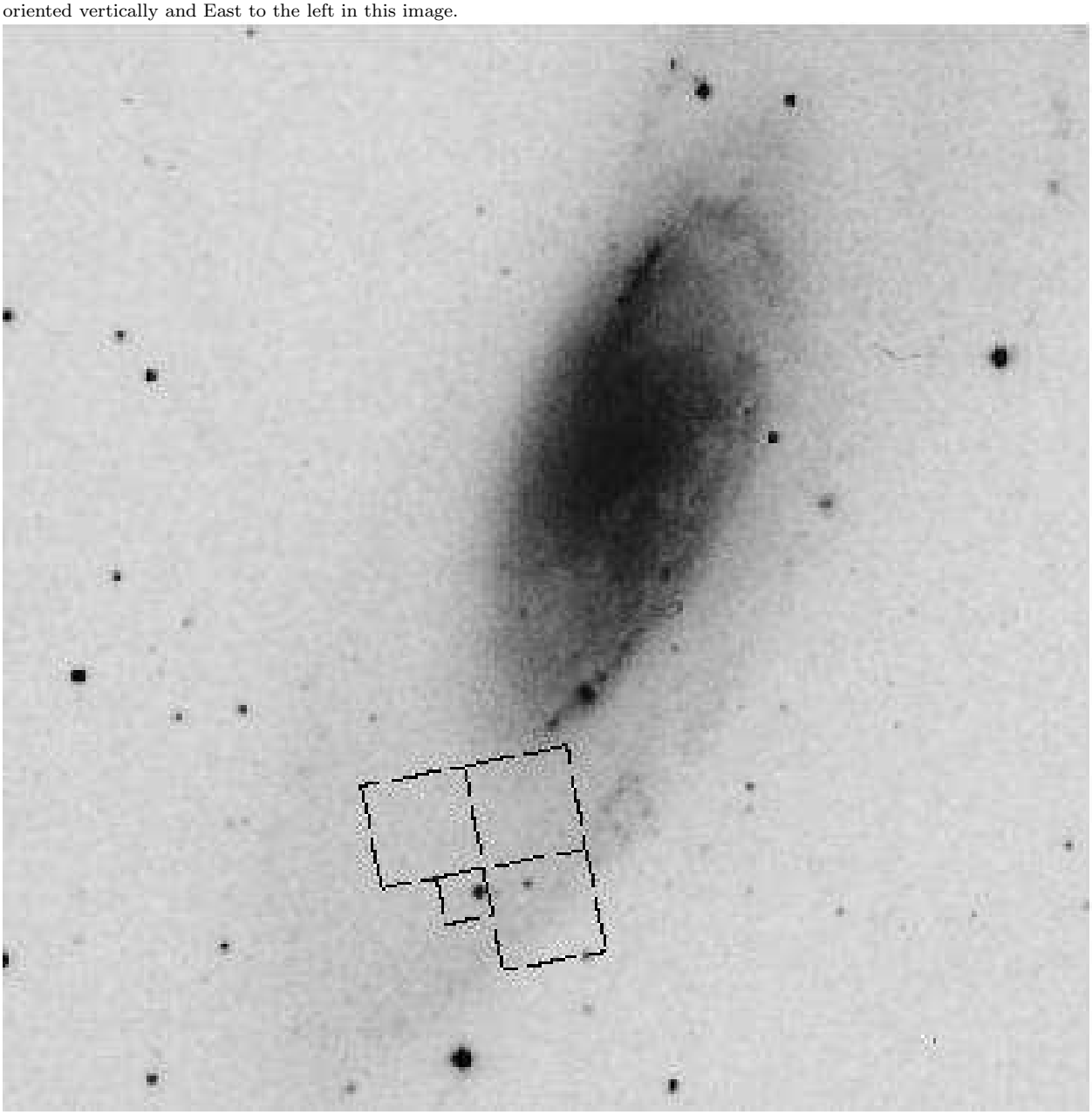

FIG. 2.— a) An image of the field covered by WF chip 2 obtained by coadding all images. The candidate Cepheids found on WF2 are circled and labelled. b) As a), but WF3 is shown.

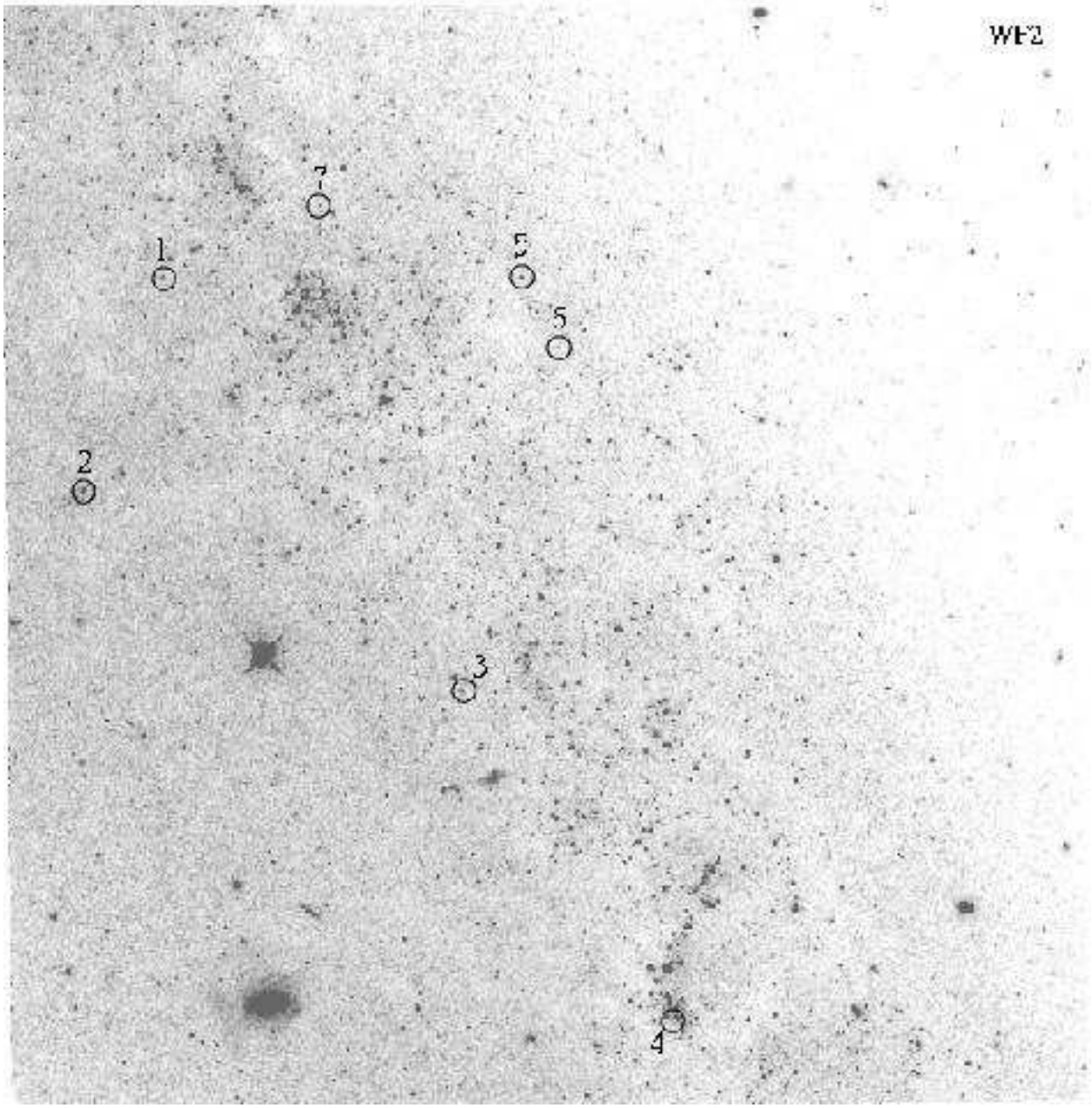

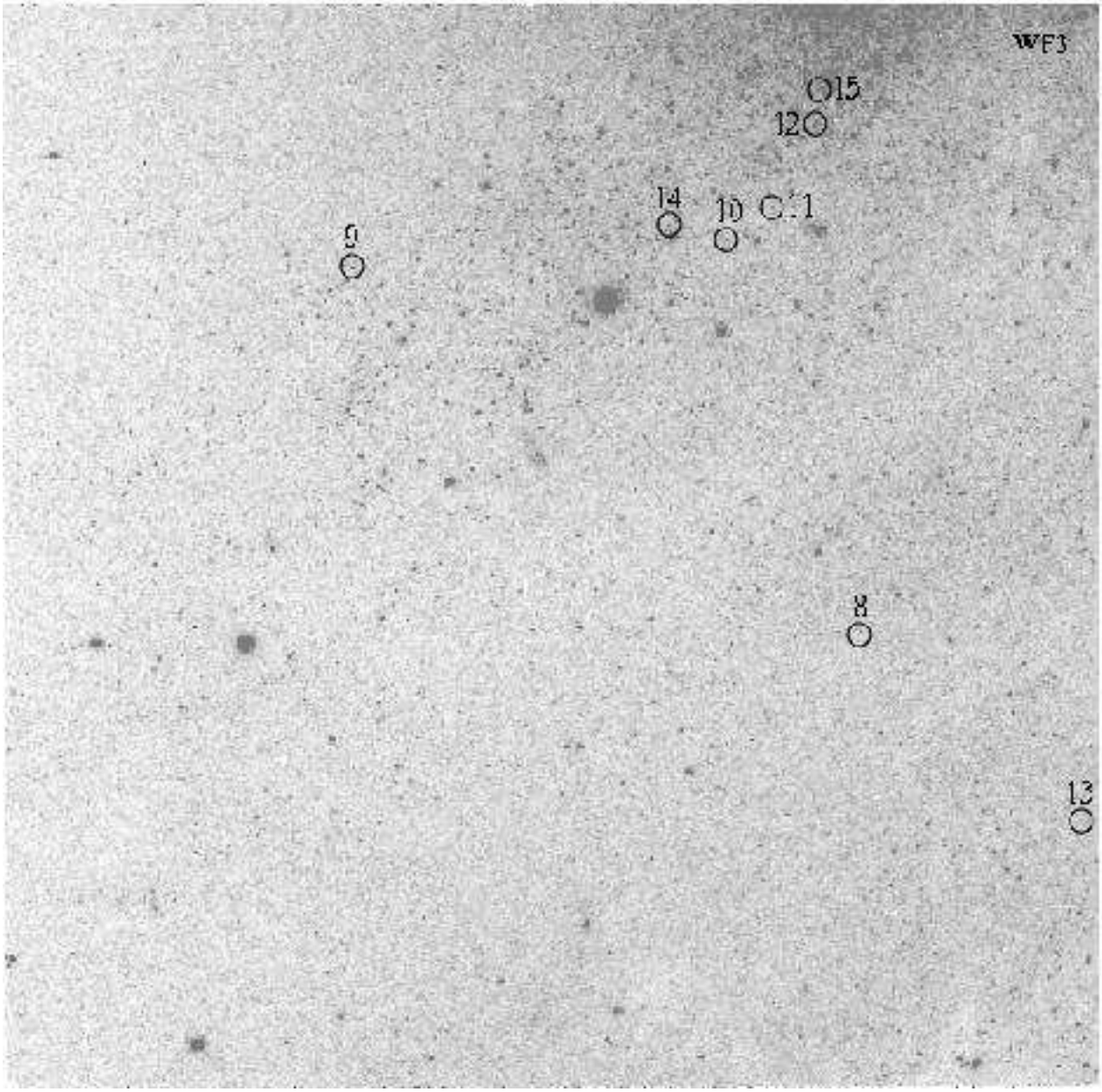
WF3
15
12
14
10
C1
9
8
13

FIG. 3.— Finding charts for the candidate Cepheids found, labelled as in Fig. 2. Each subimage shown is $7'' \times 7''$, and oriented as the images in Fig. 2.

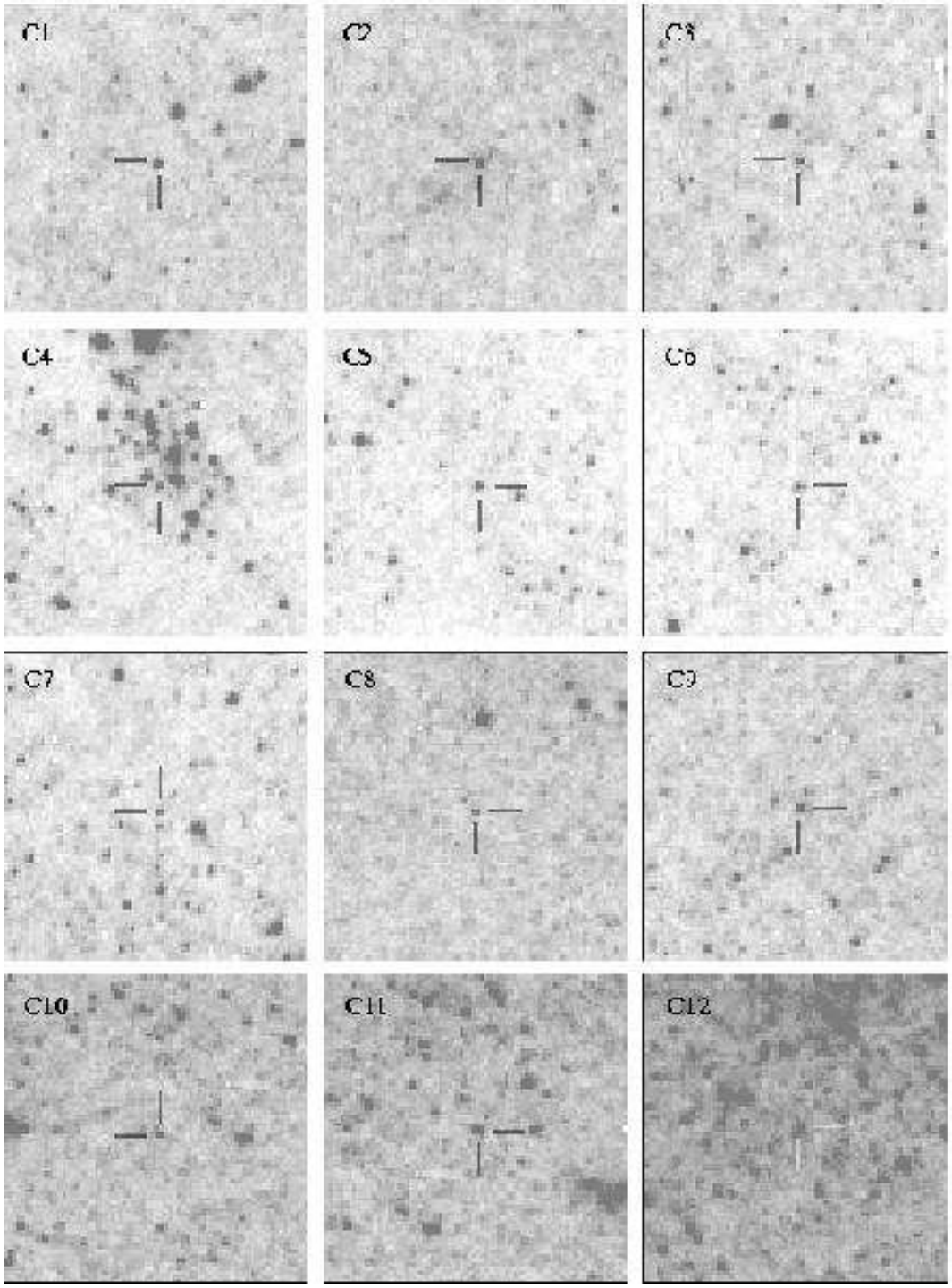

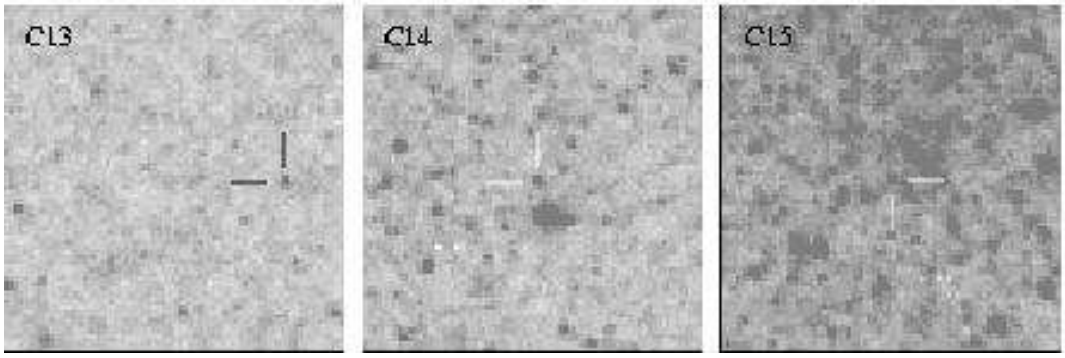
C13
C14
C15

FIG. 4.— DoPHOT $F555W$ (left) and $F814W$ (right) light curves for the candidate Cepheids found, plotted versus phase of variation. The period (in days) for each Cepheid determined during the DoPHOT analysis is also listed in its label.

FIG. 5.— (top) DoPHOT V-band Period–Luminosity relation for NGC 4258. Cepheids on WF 2 are denoted with an open diamond, those on WF 3 with a filled circle. The solid line is the best-fit P–L relation with slope as in Freedman *et al.* (2001). (bottom) As above, but based on DoPHOT I data.

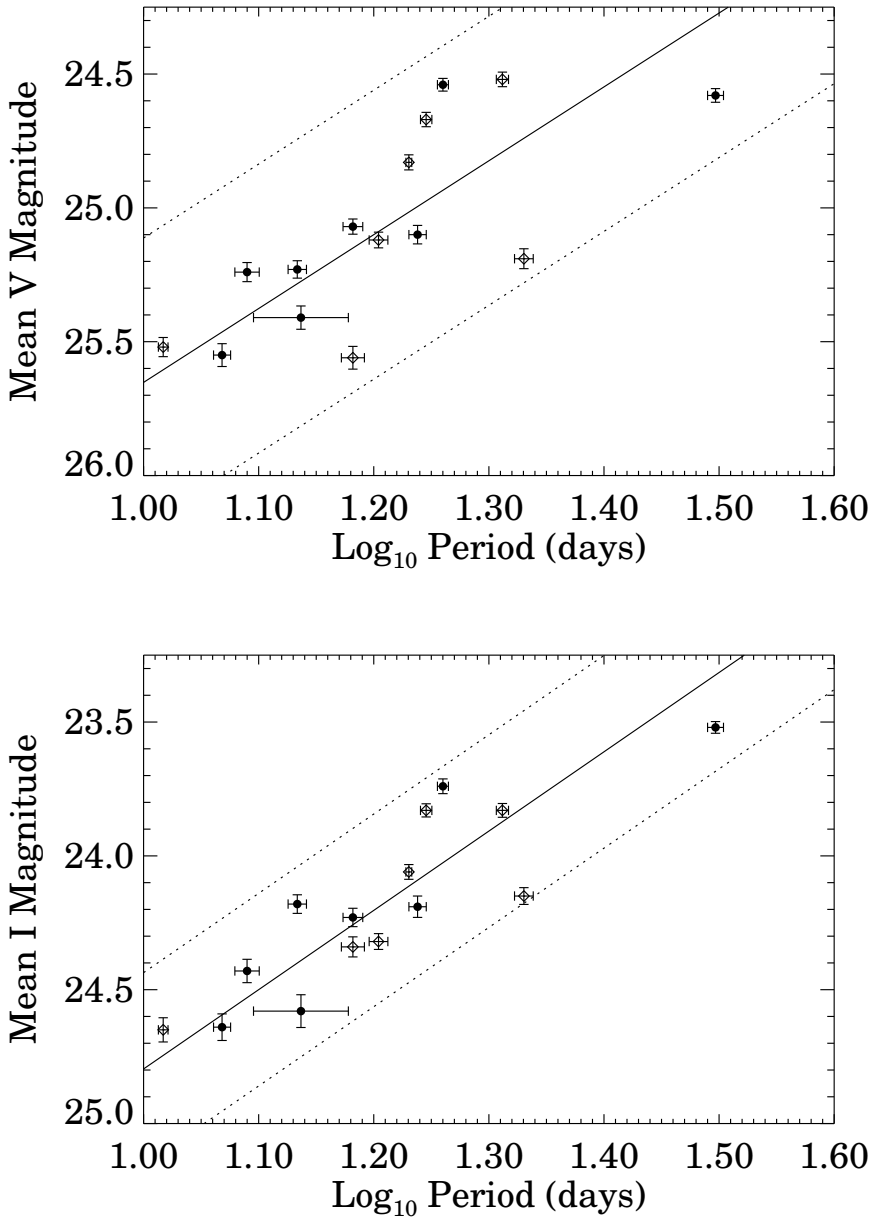

FIG. 6.— (top) ALLFRAME V-band Period–Luminosity relation for NGC 4258. Cepheids on WF 2 are denoted with an open diamond, those on WF 3 with a filled circle. The solid line is the best-fit P–L relation with slope as in Freedman *et al.* (2001). (bottom) As above, but based on ALLFRAME I data. The WF3/I discrepancy of ~ 0.06 mag cannot readily be seen on this plot.

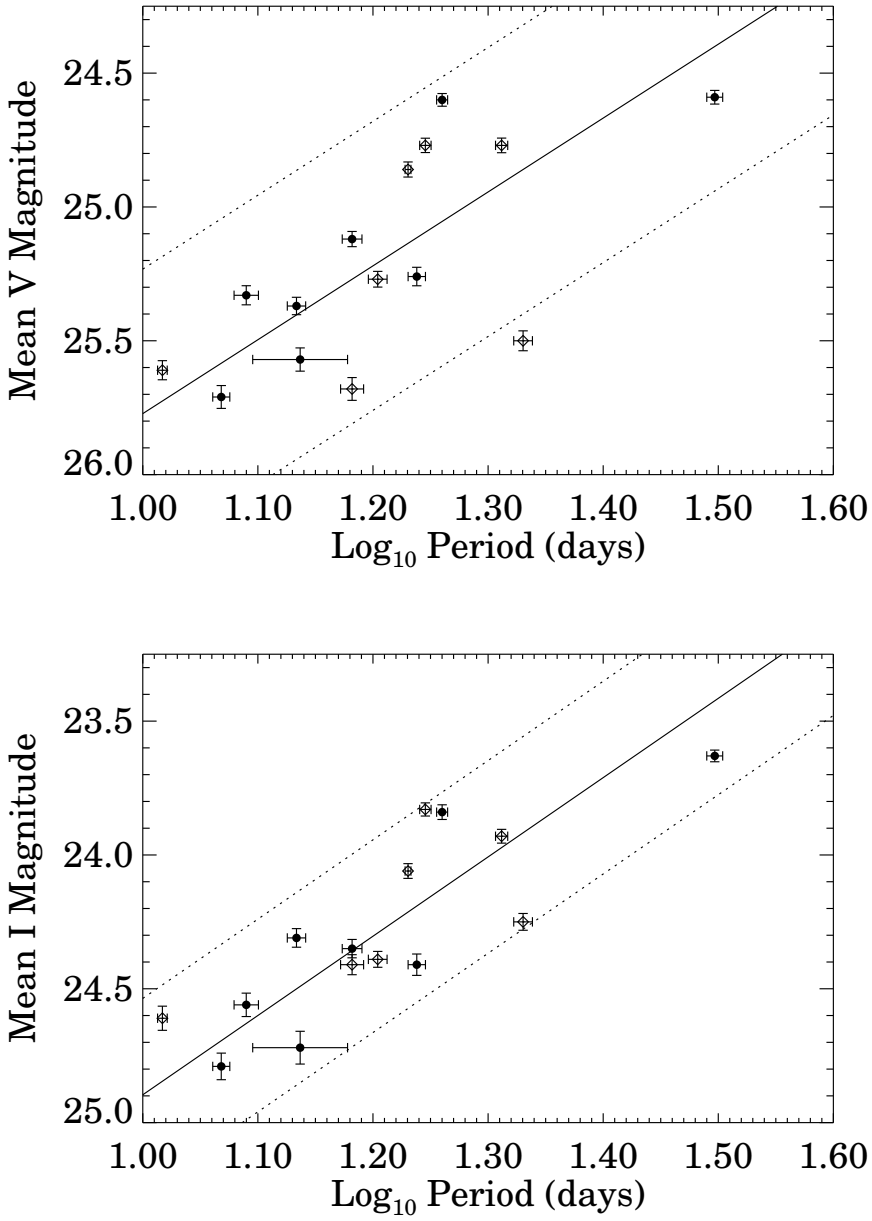

TABLE 1
JOURNAL OF OBSERVATIONS[1]

Epoch	Filter Used	Date	Julian Date[2]	Exposure Time (s)[3]	Filenames
1	F555W	1998 Apr 20	4901847.600	1000	U4F60101R/2R
	F814W		4901847.632	1000	U4F60103R/4R
2	F555W	1998 Apr 21	4901850.428	1000	U4F60201R/2R
	F814W		4901850.460	1000	U4F60203R/4R
3	F555W	1998 Apr 23	4901854.189	1000	U4F60301R/2R
	F814W		4901854.221	1000	U4F60303R/4R
4	F555W	1998 Apr 25	4901859.086	1000	U4F60401R/2R
	F814W		4901858.118	1000	U4F60403R/4R
5	F555W	1998 Apr 28	4901863.866	1000	U4F60501R/2R
	F814W		4901863.898	1000	U4F60503R/4R
6	F555W	1998 May 1	4901869.241	1000	U4F60601R/2R
	F814W		4901869.273	1000	U4F60603R/4R
7	F555W	1998 May 5	4901878.034	1000	U4F60701R/2R
	F814W		4901878.066	1000	U4F60703R/4R
8	F555W	1998 May 10	4901887.113	1000	U4F60801R/2R
	F814W		4901887.145	1000	U4F60803R/4R
9	F555W	1998 May 15	4901897.864	1000	U4F60901R/2R
	F814W		4901897.896	1000	U4F60903R/4R
10	F555W	1998 May 22	4901912.376	1000	U4F61001R/2R
	F814W		4901912.408	1000	U4F61003R/4R
11	F555W	1998 May 30	4901928.500	1000	U4F61101R/2R
	F814W		4901928.532	1000	U4F61103R/4R

[1]For all observations, the WFPC2 camera was used centered on R.A. $12^h\ 19^m\ 8.95^s$, declination $47^d\ 13^m\ 26.76^s$ (J2000), with roll angle 325.9943

[2]Heliocentric; at midpoint of the two exposures

[3]Total of two exposures

TABLE 2
PARAMETERS OF CEPHEIDS FOUND

				DoPHOT				ALLFRAME		
ID	Chip	X[1]	Y[1]	$< V >^2$	$< I >^2$	Period (d)	Amplitude[3]	$< V >^2$	$< I >^2$	Period (d)
C1	2	158.18	603.73	24.55 ± 0.03	23.84 ± 0.03	20.5 ± 0.2	1.08	24.77	23.94	21.3
C2	2	102.72	455.97	24.70 ± 0.03	23.84 ± 0.02	17.6 ± 0.2	0.99	24.77	23.84	17.2
C3	2	364.28	317.39	24.86 ± 0.03	24.07 ± 0.03	17.0 ± 0.1	1.14	24.86	24.07	17.0
C4	2	509.26	90.23	25.22 ± 0.04	24.16 ± 0.03	21.4 ± 0.4	1.00	25.50	24.26	20.5
C5	2	405.30	604.14	25.15 ± 0.03	24.33 ± 0.03	16.0 ± 0.3	0.68	25.27	24.40	14.0
C6	2	431.21	554.94	25.59 ± 0.04	24.35 ± 0.04	15.2 ± 0.3	0.74	25.68	24.42	13.9
C7	2	447.29	566.43	25.55 ± 0.04	24.66 ± 0.05	10.4 ± 0.1	0.79	25.61	24.62	10.1
C8	3	627.67	365.75	25.58 ± 0.04	24.65 ± 0.05	11.7 ± 0.2	0.60	25.71	24.80	11.2
C9	3	276.75	618.19	25.10 ± 0.03	24.24 ± 0.03	15.2 ± 0.3	0.95	25.12	24.36	15.2
C10	3	535.47	636.44	25.13 ± 0.03	24.20 ± 0.04	17.3 ± 0.3	0.81	25.26	24.42	17.6
C11	3	566.89	659.25	24.61 ± 0.03	23.53 ± 0.02	31.4 ± 0.5	0.82	24.59	23.64	30.7
C12	3	597.51	717.16	24.57 ± 0.02	23.75 ± 0.03	18.2 ± 0.2	0.93	24.60	23.85	17.6
C13	3	780.74	236.12	25.27 ± 0.04	24.44 ± 0.04	12.3 ± 0.3	0.97	25.33	24.57	12.4
C14	3	495.77	645.99	25.26 ± 0.03	24.19 ± 0.03	13.6 ± 0.2	0.74	25.37	24.32	13.7
C15	3	599.59	740.72	25.44 ± 0.04	24.59 ± 0.06	13.7 ± 1.3	0.82	25.57	24.73	13.0

[1]In the coordinate system of the first $F555W$ exposure, U4F60101R

[2]Intensity-weighted mean magnitudes are given for DoPHOT; for ALLFRAME, intensity-weighted means based on the template fits are listed

[3]Peak-to-peak, in magnitudes, based upon template fit

TABLE 3
DoPHOT Photometry of Cepheids Found

Epoch	C1	C2	C3	C4	C5
			V		
1	25.07±0.10	25.26±0.11	25.12±0.10	24.97±0.07	25.27±0.09
2	24.11±0.05	24.99±0.10	25.27±0.12	24.99±0.09	24.80±0.08
3	24.06±0.04	24.10±0.08	25.41±0.11	25.07±0.10	24.73±0.06
4	24.33±0.06	24.46±0.08	25.30±0.10	25.13±0.09	25.15±0.08
5	24.52±0.06	24.58±0.06	24.31±0.06	25.56±0.12	25.27±0.11
6	24.70±0.08	24.82±0.08	24.47±0.12	26.02±0.18	25.60±0.12
7	25.09±0.09	25.41±0.11	24.72±0.08	25.77±0.12	25.20±0.11
8	...	24.72±0.09	25.40±0.12	24.75±0.07	...
9	24.34±0.09	24.55±0.06	24.25±0.08	25.44±0.12	25.40±0.10
10	24.76±0.08	25.22±0.10	24.91±0.09	25.99±0.15	25.09±0.08
11	25.24±0.09	24.38±0.06	25.20±0.11	24.69±0.07	25.30±0.10
			I		
1	24.25±0.13	24.15±0.08	23.95±0.09	23.95±0.08	24.34±0.09
2	23.75±0.07	23.95±0.08	24.16±0.10	24.05±0.09	24.34±0.09
3	23.48±0.08	23.63±0.08	24.24±0.09	23.95±0.08	24.06±0.10
4	23.74±0.09	23.50±0.10	24.38±0.12	24.10±0.09	24.32±0.10
5	23.73±0.08	23.70±0.08	23.80±0.07	24.27±0.08	24.39±0.11
6	23.83±0.09	23.87±0.08	24.06±0.12	24.61±0.13	24.49±0.10
7	23.97±0.09	24.07±0.08	23.96±0.09	24.77±0.12	24.40±0.10
8	24.20±0.09	23.82±0.07	24.42±0.12	23.92±0.07	24.05±0.08
9	23.52±0.06	23.79±0.08	23.67±0.07	24.07±0.08	24.75±0.12
10	23.90±0.07	24.14±0.09	23.94±0.08	24.65±0.11	24.23±0.08
11	24.09±0.08	23.48±0.08	24.50±0.12	23.91±0.06	24.39±0.13

TABLE 3
DoPHOT Photometry of Cepheids Found

Epoch	C6	C7	C8	C9	C10
			V		
1	25.32±0.10	25.56±0.14	25.57±0.13	24.77±0.08	24.64±0.06
2	25.28±0.11	25.87±0.15	25.51±0.11	24.84±0.08	24.78±0.08
3	25.35±0.11	25.62±0.11	25.95±0.17	25.07±0.08	25.02±0.08
4	25.79±0.15	25.23±0.09	25.77±0.17	25.34±0.11	25.07±0.09
5	26.07±0.18	25.25±0.10	25.24±0.10	25.60±0.15	25.47±0.15
6	25.91±0.13	25.94±0.17	25.37±0.11	25.16±0.10	25.43±0.12
7	25.30±0.09	25.60±0.11	25.98±0.19	24.63±0.06	25.41±0.13
8	25.67±0.13	25.55±0.12	25.33±0.10	25.31±0.09	24.92±0.12
9	25.88±0.16	25.46±0.10	25.78±0.14	25.33±0.11	25.37±0.10
10	25.30±0.13	25.86±0.17	25.37±0.12	24.96±0.09	25.50±0.12
11	26.06±0.16	25.37±0.12	25.85±0.18	25.60±0.14	25.18±0.14
			I		
1	24.41±0.11	24.46±0.14	24.51±0.14	24.20±0.11	24.05±0.10
2	24.28±0.12	24.84±0.18	24.69±0.17	23.81±0.09	23.90±0.08
3	24.20±0.13	24.89±0.15	24.82±0.18	24.18±0.10	24.04±0.10
4	24.36±0.13	24.53±0.13	24.61±0.15	24.24±0.12	24.07±0.10
5	24.24±0.12	24.55±0.11	24.60±0.15	24.70±0.18	24.30±0.12
6	24.63±0.15	24.82±0.18	24.42±0.12	24.49±0.13	24.55±0.14
7	24.14±0.10	24.55±0.12	25.01±0.23	24.13±0.11	24.46±0.14
8	24.20±0.11	24.78±0.16	24.31±0.13	24.13±0.09	23.94±0.11
9	24.81±0.15	24.46±0.14	25.13±0.22	24.59±0.13	24.26±0.11
10	24.39±0.12	24.73±0.20	24.59±0.17	24.15±0.10	24.61±0.17
11	24.36±0.11	24.78±0.21	24.73±0.16	24.37±0.13	24.29±0.14

TABLE 3
DoPHOT Photometry of Cepheids Found

Epoch	C11	C12	C13	C14	C15
			V		
1	24.83±0.14	24.89±0.11	24.82±0.10	25.50±0.16	25.16±0.11
2	24.86±0.08	24.87±0.08	25.10±0.09	25.11±0.09	25.16±0.10
3	24.95±0.09	24.95±0.08	25.32±0.12	24.76±0.09	25.29±0.11
4	24.87±0.09	24.95±0.08	25.80±0.14	25.00±0.08	25.69±0.17
5	25.01±0.10	24.04±0.06	25.52±0.12	25.27±0.12	26.04±0.24
6	24.47±0.08	24.37±0.09	24.80±0.08	25.43±0.12	25.49±0.14
7	24.02±0.08	24.57±0.08	25.35±0.10	25.52±0.10	25.24±0.11
8	24.17±0.08	24.94±0.09	25.77±0.15	25.32±0.10	25.90±0.17
9	24.54±0.06	23.89±0.05	24.97±0.08	25.70±0.14	25.37±0.13
10	24.78±0.07	24.63±0.08	25.88±0.16	25.02±0.08	25.79±0.15
11	24.72±0.08	24.88±0.11	25.33±0.12	25.68±0.12	25.17±0.11
			I		
1	23.71±0.09	24.03±0.11	24.47±0.17	24.30±0.12	24.25±0.14
2	23.53±0.09	23.96±0.10	24.33±0.13	24.16±0.10	24.54±0.16
3	23.79±0.07	24.10±0.12	24.64±0.16	23.95±0.10	24.35±0.13
4	23.74±0.07	23.57±0.09	24.72±0.15	24.00±0.12	24.75±0.22
5	23.77±0.07	23.36±0.07	24.56±0.14	24.36±0.14	25.03±0.26
6	23.44±0.06	23.58±0.08	24.16±0.11	24.24±0.12	24.98±0.25
7	23.33±0.09	23.77±0.08	24.12±0.13	24.18±0.11	24.52±0.17
8	23.22±0.05	23.97±0.11	24.77±0.17	24.12±0.11	...
9	23.37±0.06	23.39±0.07	24.46±0.16	24.49±0.14	24.41±0.13
10	23.59±0.07	23.94±0.12	24.54±0.17	24.18±0.10	...
11	23.60±0.06	23.86±0.10	24.29±0.12	24.23±0.13	24.43±0.17

TABLE 4
NGC 4258 DISTANCE MODULI (NO METALLICITY CORRECTION)

Photometry Used	Subset of Cepheids	μ_V (mag)	μ_I (mag)	μ_0 (mag)
DoPHOT	All	29.90 ± 0.07	29.69 ± 0.05	**29.40 ± 0.06**
	Chip 2	29.92 ± 0.13	29.72 ± 0.085	29.43 ± 0.10
	Chip 3	29.87 ± 0.10	29.67 ± 0.06	29.38 ± 0.07
ALLFRAME	All	29.99 ± 0.075	29.80 ± 0.05	**29.53 ± 0.07**
	Chip 2	30.03 ± 0.14	29.77 ± 0.09	29.40 ± 0.10
	Chip 3	29.97 ± 0.08	29.84 ± 0.07	29.65 ± 0.09
Corrected ALLFRAME	All	29.99 ± 0.075	29.77 ± 0.05	**29.44 ± 0.06**
	Chip 2	30.03 ± 0.14	29.77 ± 0.09	29.40 ± 0.10
	Chip 3	29.97 ± 0.08	29.77 ± 0.07	29.48 ± 0.09

Table 5
Uncertainties in This Distance Measurement

	Source	Error
S_1	Systematic Errors in LMC P-L Calibration	
	A. LMC True Modulus	±0.10
	B. LMC P-L Zero Point	±0.02
	A and B added in quadrature	±0.10
S_2	Systematic Errors in WFPC2 Zero Points	±0.07
S_3	Average Metallicity Correction	±0.08
S_4	Systematic Errors Unique to NGC 4258 Photometry	±0.05
S_5	Dependence of NGC 4258 Distance Modulus on Magnitude Averaging Method	±0.04
R_1	Random Error in the NGC 4258 Extinction-Corrected Distance Modulus	
	C. NGC 4258 P-L Fit (V)	±0.07
	D. NGC 4258 P-L Fit (I)	±0.05
	C and D partially correlated	±0.06
R_{tot}	Errors Only Affecting This Determination (S_4, S_5, and R_1 added in quadrature)	**±0.09**
S_{tot}	Systematic Errors in Key Project Techniques (S_1, S_2, and S_3 added in quadrature)	**±0.15**

This figure "fig2a.png" is available in "png" format from:

http://arXiv.org/ps/astro-ph/0012377v1

This figure "fig2b.png" is available in "png" format from:

http://arXiv.org/ps/astro-ph/0012377v1

This figure "fig4a.png" is available in "png" format from:

http://arXiv.org/ps/astro-ph/0012377v1

This figure "fig4b.png" is available in "png" format from:

http://arXiv.org/ps/astro-ph/0012377v1

This figure "fig4c.png" is available in "png" format from:

http://arXiv.org/ps/astro-ph/0012377v1

This figure "fig4d.png" is available in "png" format from:

http://arXiv.org/ps/astro-ph/0012377v1